https://doi.org/10.5194/egusphere-2023-653
Preprint. Discussion started: 11 April 2023

Extremely Warm European Summers driven by Sub-Decadal North Atlantic Heat Inertia

Lara Hellmich[1,2], Laura Suarez-Gutierrez[1,3,4], Daniela Matei[1], and Wolfgang A. Müller[1]

[1]Max Planck Institute for Meteorology, Hamburg, Germany
[2]International Max Planck Research School on Earth System Modelling (IMPRS-ESM), Hamburg, Germany
[3]Institute of Atmospheric and Climate Science, ETH Zürich, Zurich, Switzerland
[4]Institut Pierre-Simon Laplace, CNRS, Paris, France

Correspondence: Lara Hellmich (lara.hellmich@mpimet.mpg.de)

Abstract. The internal variability of European summer temperatures has been linked to various mechanisms on seasonal to sub- and multi-decadal timescales. We find that sub-decadal time scales dominate summer temperature variability over large parts of the continent, and the mechanisms controlling such sub-decadal variations remain unexplored. Extremely warm summers occurring in sub-decadal periods when abnormally warm summer temperatures conglomerate are controlled by a strengthening of the subtropical gyre, an increase of heat transport, and an accumulation of heat content several years prior to an extremely warm European summer, thereby affecting ocean-atmosphere heat fluxes during extreme summers. This leads to a weakening and northward displacement of the jet stream and increased probability of atmospheric blocking over Scandinavia. Our findings link the occurrence of extremely warm European summers to the inertia of the North Atlantic, whose potential to improve the predictability of extremely warm summers several years ahead is of great societal interest, especially in a warming climate.

1 Introduction

Extremely warm European summers have an increasingly large societal impact. Extreme temperatures can lead to severe health problems and are thus associated with an increased mortality (Gasparrini et al., 2015; Vicedo-Cabrera et al., 2021). Furthermore, heat extremes can also lead to economic impacts, such as crop failure and water shortage (Ribeiro et al., 2020), and political aspects, such as climate migration and general crisis management (Ceglar et al., 2019). European summers will become more extreme in a warming climate due to rising mean temperatures (Seneviratne et al., 2021) and also due to an increase in variability (Schär et al., 2004; Fischer et al., 2012; Suarez-Gutierrez et al., 2020a). Moreover, when such extreme summers occur repeatedly year after year, they become even more threatening to the already vulnerable socioeconomic and ecological resilience of the region (Ruiter et al., 2020; Callahan and Mankin, 2022).

On time scales of days to several weeks, the main drivers of extreme heat are soil moisture deficits and moisture-temperature feedbacks (Seneviratne et al., 2006; Fischer and Schär, 2008; Vogel et al., 2017; Suarez-Gutierrez et al., 2020a) and large-scale atmospheric patterns such as atmospheric blocking and the North Atlantic Oscillation as parts of the large-scale atmospheric circulation (Meehl and Tebaldi, 2004; Horton et al., 2015; Li et al., 2020; Suarez-Gutierrez et al., 2020a). However, these short-term drivers of extreme temperatures could be influenced and conditioned by mechanisms on longer time scales. Long

https://doi.org/10.5194/egusphere-2023-653
Preprint. Discussion started: 11 April 2023

memory mechanisms such as ocean heat inertia, i.e., the capacity to store heat and delay its transfer and release, have been found to influence mean summer temperatures (Saeed et al., 2013; Ghosh et al., 2016; Borchert et al., 2019), in detail such as by the Atlantic multi-decadal variability (AMV; Gao et al., 2019; Qasmi et al., 2021) or the El-Nino Southern Oscillation (ENSO; Martija-Díez et al., 2021). The variability in the North Atlantic region for different ocean-related quantities indicates that a fully coupled atmosphere-ocean cycle with a period of about 7-10 years (Reintges et al., 2016; Martin et al., 2019) and decadal processes in the North Atlantic have a significant impact on European summer temperatures (Müller et al., 2020). However, neither have the drivers for extreme temperatures on long-term timescales been extensively assessed, nor do we know which year to multi-year timescales are most relevant for extreme summers. In this study, we answer these questions and provide a mechanism explaining how North Atlantic heat inertia drives extremely warm European summers years in advance.

We focus on extreme European summers occurring in multi-year periods of abnormally warm temperatures. To robustly capture the frequency and strength of such low-probability events, large sample sizes are needed. Here, we use the largest ensemble from a comprehensive, fully coupled Earth system model currently available, the Max-Planck-Institute Grand Ensemble with 100 ensemble members (MPI-GE; Maher et al., 2019). MPI-GE offers one of the best representations of observed historical temperatures of all available single-model initial condition large ensembles (SMILES; Suarez-Gutierrez et al., 2021). Additionally, MPI-GE is able to capture extreme summer temperatures (Suarez-Gutierrez et al., 2020b), including some of the most extreme European summers (Suarez-Gutierrez et al., 2018, 2020a).

Using the MPI-GE, we examine the sub-decadal variability of extremely warm European summers and show how these summers are affected by North Atlantic heat inertia. Doing so, we confirm that the MPI-GE can represent sub-decadal temperature variability well, and identify where these time scales dominate over Europe and are linked to European extreme temperatures. Additionally, we identify which processes in the North Atlantic increase the occurrence of extremely warm summers. A link between North Atlantic heat inertia and extremely warm European summers helps to improve the predictability of temperature and associated heat extremes by identifying periods that increase the likelihood of extremely warm summers several years in advance.

2 Data and Methods

2.1 Model Description

We use simulations from the Max Planck Institute Grand Ensemble (MPI-GE; Maher et al., 2019). These simulations are done with MPI-ESM1.1 in the low-resolution setup (MPI-ESM-LR; Mauritsen et al., 2012; Giorgetta et al., 2013). MPI-GE consists of 100 simulations with different initial conditions and is one of the largest ensembles of a single, comprehensive, fully-coupled climate model. In the atmosphere, the MPI-ESM-LR reaches up to 0.01 hPa (about 80 km) with 47 vertical levels and a horizontal resolution of 200km at the equator. In the ocean, the MPI-ESM-LR has 40 vertical levels and a horizontal resolution of 12-150km. Here, we focus on summer means (JJA) from 1950 to 2022. This includes historical simulations from 1950 to 2005 and RCP4.5 scenario simulations until 2022 (for time-lagged analyses years prior to 1950 are analyzed).

https://doi.org/10.5194/egusphere-2023-653
Preprint. Discussion started: 11 April 2023

ERA5 data including the backward extension until 1950 are used as an observational reference to validate the results of the multi-tapering with MPI-GE (Hersbach et al., 2018). ERA5 data are regridded to the coarser MPI-ESM-LR grid.

2.2 Analysis Methods

Multi-Taper Method: We use a cross-spectral analysis, which is performed by using the multi-taper method as described by Årthun et al. (2018), to analyze if and where the MPI-GE can represent the sub-decadal time scales well. We perform the multi-tapering for all 100 ensemble members and each grid point to ascertain the dominant timescale (e.g. Årthun et al., 2018; Ghil et al., 2002). Doing so, the dominant timescale is given by the highest significant peak. The significance of spectral peaks is determined by comparison with a red noise spectrum with a 95% confidence interval around the red noise.

Detrending and Bandpass-Filtering: We detrend all of our data in order to exclude the influence of global warming and other external forcings, therefore we use the Climate Data Operators (CDO) command "detrend" (von Storch and Zwiers, 1984). Furthermore, we use a 5-10 year bandpass filter to remove frequencies and noise outside the sub-decadal range. Therefore, we use a standard top-hat filter response function which is also implemented in the CDO toolkit.

Determination of Significance: The significance of our results is tested with a bootstrap algorithm in which a reference index is computed in each grid point for 1000 randomly composed arrays (random sampling with replacement). We then construct a 95%-confidence interval from the 0.025- and 0.975-quantiles of our 1000 bootstraps and consider a value significant once the null hypothesis falls outside this confidence interval.

Scaled Anomalies within Figure Captions: To better illustrate the imprint of the sub-decadal proportion of various climate variables on the occurrence of extremely warm European summers, we scale the band-pass filtered summer mean anomalies by the total summer mean variability during extremely warm European summers. In detail, we first calculate anomalies of the variables with respect to their long-term averages. We then define their total summer mean variability as the standard deviation of the unfiltered summer mean anomaly for times when heat extremes occur. At the time of each heat extreme, we then divide the bandpass-filtered anomaly by the total variability. Lastly, we average over all cases of extreme events to obtain the scaled anomaly. All calculations of the scaled anomaly are performed gridpoint-wise. The scaled anomaly simply illustrates the proportion that a sub-decadal mean change has on the occurrence of an heat extreme compared to the overall occurrence of heat extremes. The corresponding scaled anomalies are added to the respective figure captions.

$$\text{During extremely warm European summers: } \frac{\text{bandpass-filtered anomaly}}{\text{standard deviation of total variability}}$$

3 Results

3.1 Sub-Decadal Variability and Extremely Warm European Summers

We use bandpass-filtering and a cross-spectral analysis to identify the dominant time-frequencies of European summer temperatures for each grid point in MPI-GE and ERA5 from 1950 to 2020 (Fig. 1a,b and Methods). Areas with dominant sub-decadal variations (5-10 year variations) are found in MPI-GE over Scandinavia, the British Isles, the Iberian Peninsula, Italy, and large

https://doi.org/10.5194/egusphere-2023-653
Preprint. Discussion started: 11 April 2023

parts of Central and Eastern Europe. ERA5 and MPI-GE show high agreement for areas with dominant sub-decadal variations especially over Eastern Europe (Fig. 1a,b). MPI-GE reveals some limitations in the representation of multi-decadal time scales (>20 years), which are dominant in ERA5 in the northern and southernmost parts of the domain. Also, timescales between 10 and 20 years are dominant in only a few more grid points compared to timescales above 20 years.

The dominant sub-decadal time scales are linked to the occurrence of extremely warm European summers. To identify extremely warm European summers occurring in abnormally warm periods, we choose temperature anomalies above the 90th percentile coinciding with a positive phase of the 5-10 year bandpass-filtered temperature. Central Europe stands out as the area with the largest number of extremely warm summers occurring on sub-decadal time scales per grid point (Fig. 1c). Regions within the Iberian Peninsula, northern Scandinavia, and Russia also stand out with coinciding extremely warm summers and sub-decadal variability. In summary, sub-decadal timescales of 5-10 years are the dominant scale of variability in European mean summer temperatures, and extremely warm summers tend to occur in 5-10 year phases of abnormally warm temperatures over Europe over large parts of Central, Eastern and Southern Europe.

The overlap between a dominant sub-decadal variability and the occurrence of extremely warm European summers is strongest over Central Europe, which we define as an area of 15°-35°E; 45°-60°N (Fig. 1c, blue box). The temperature of this region is also dominated by the sub-decadal time scales overall (Fig. 1d), as expected from Fig. 1b, two significant peaks within the sub-decadal time scales can be found here as well. To further understand this simultaneous occurrence of sub-decadal variability and extremely warm European summers, and its drivers, we investigate the behaviour of several variables that characterize the North Atlantic heat variability during extremely warm European summers as well as several years prior.

https://doi.org/10.5194/egusphere-2023-653
Preprint. Discussion started: 11 April 2023

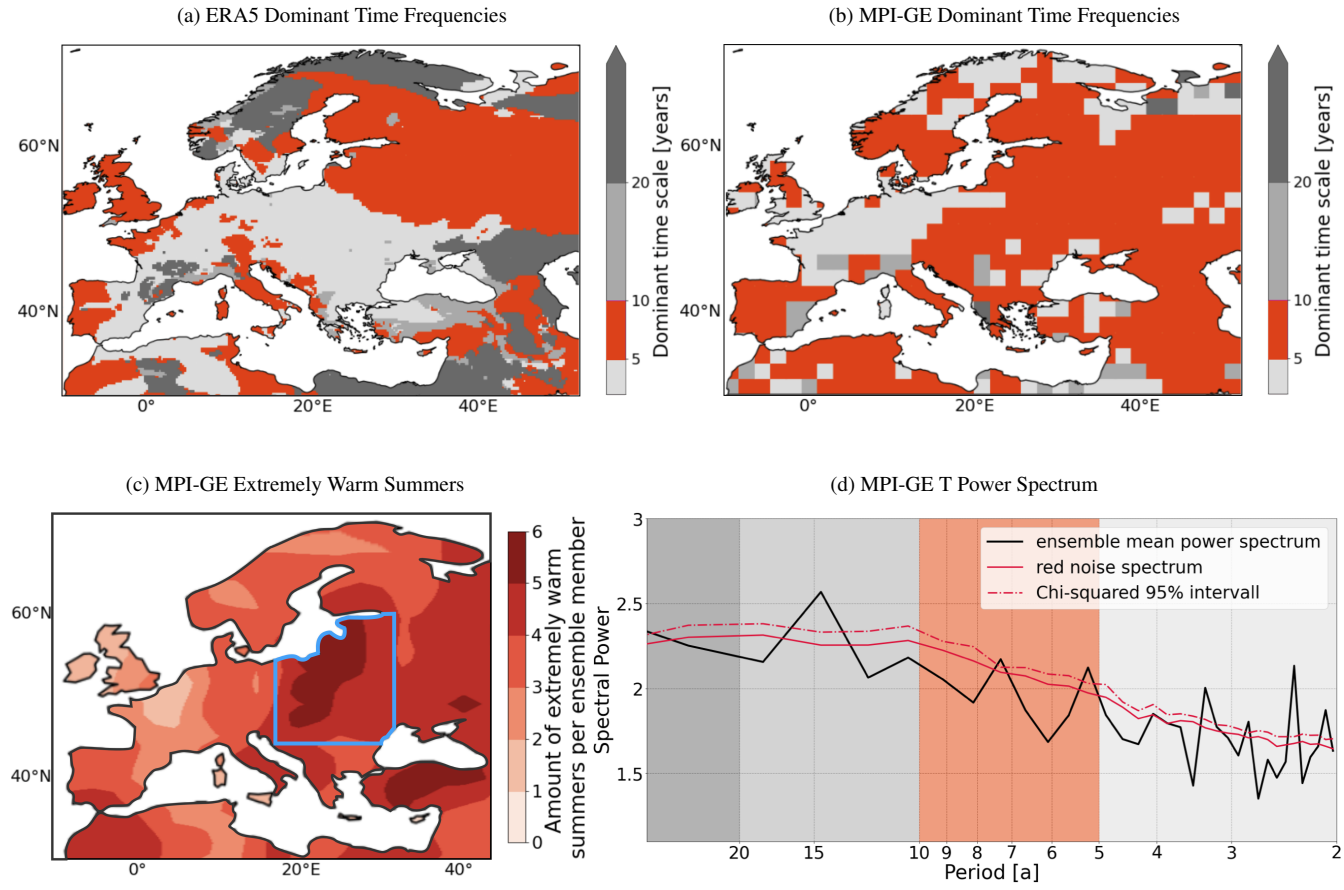

Figure 1. Dominant time frequencies and their relation to extremely warm European summersheat extremes. (a),(b) Cross-spectral analysis, performed using the multi-taper method, showing the dominant time scales of European surface air temperature variability in (a) ERA5 and (b) MPI-GE (see Methods). Color shading in years. (c) Amount of extremely warm European summers on sub-decadal time scales (T > 90th perc. and T$bandpass$ > 0) in MPI-GE. The blue box defines the region of interest for further analysis (Central Europe, ∼15°-35°E; 45°-60°N). (d) Power spectrum of Central European (spatial mean of blue box) surface air temperature (black line) in MPI-GE (averaged over all ensemble member spectra). The significance is shown via a red-noise spectrum (solid red line) and the chi-squared 95% interval (dashed red line). The background is color-coded according to the time intervals in (a,b). Period 1950-2022.

3.2 The North Atlantic Ocean and Extremely Warm European Summers

To find out how the North Atlantic long-term variability could drive the sub-decadal variability in extremely warm European summers found in Fig. 1, we investigate the North Atlantic ocean-atmosphere latent and sensible heat fluxes happening concurrently and years prior to an extreme summer (Fig. 2a).

At lag 0, when anomalies in the North Atlantic occur in the same year as the extreme summer, we find high anomalies, reaching up to 20% of the total variability, in the western part of the North Atlantic (30°-60°W; 25°-40°N), as well as in the

https://doi.org/10.5194/egusphere-2023-653
Preprint. Discussion started: 11 April 2023

north-eastern part of the North Atlantic (15°-25°W; 50°-70°N). These high anomalies in the North Atlantic, which indicate an above-average heat flux from the ocean to the atmosphere during extremely warm European summers and associated warming of the atmosphere, can be traced to years prior to the extreme.

Although the global anomaly pattern suggests some relation to other long-term climate variability modes over the Pacific (Fig. 2b), further analysis shows that e.g. ENSO does not drive the mechanism described here (Table A1). This means in detail, that the fraction of extremely warm European summers during the different ENSO phases (El-Nino, La-Nina, Neutral) is consistently low for different lags, so that no specific ENSO phase can be concretely linked to extremely warm European summers on sub-decadal time scales. On the contrary, the proportion of extremely warm European summers is strongly dependent on the state of oceanic variables of the North Atlantic. Although this connection could be coincidental and caused by a third-party process (Cane et al., 2017), this response could also indicate a causal relationship.

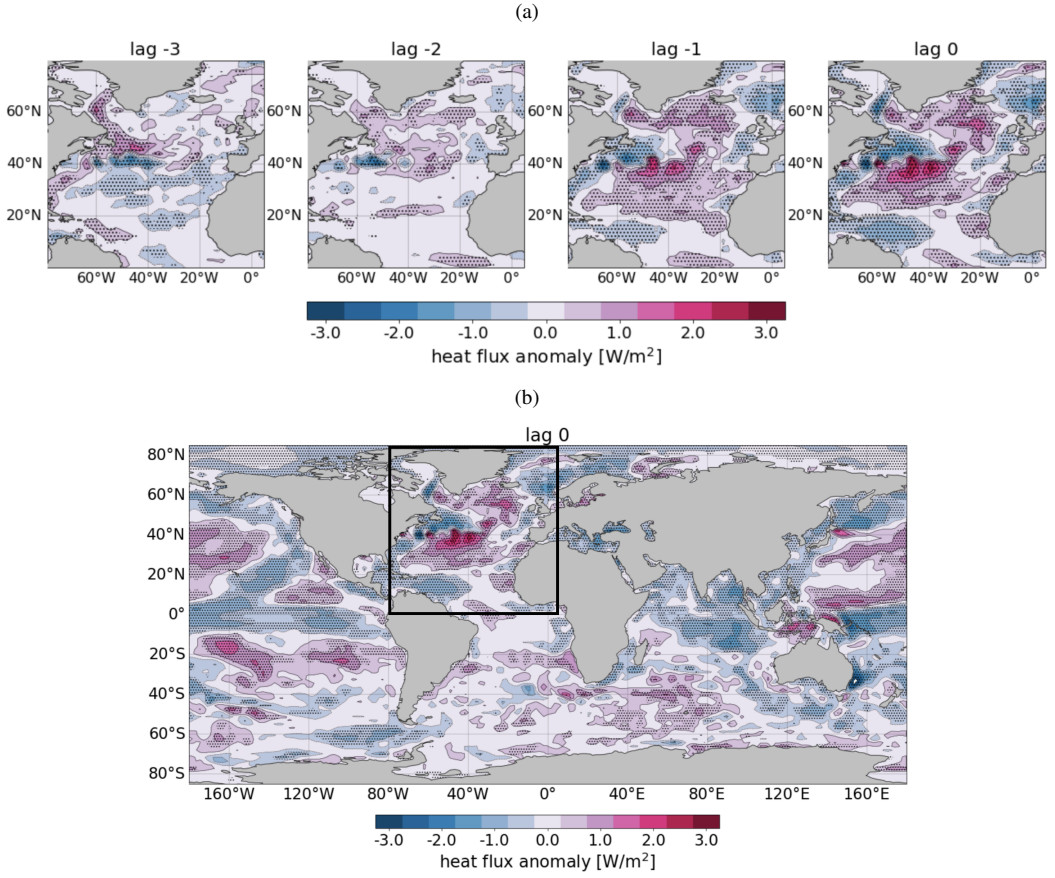

Figure 2. Anomaly of 5-10 year bandpass-filtered Atlantic heat flux (latent + sensible) variability in MPI-GE for (a) different lags prior to extremely warm European summers and (b) lag 0 as a global map. Positive values indicate heat flux into the atmosphere. Values in Wm^{-2}, lags in years. Dots denote significance at a 95% confidence level. Period 1950-2022. For comparison the standard deviation of the year-to-year variation is of the order of $14\,\mathrm{Wm}^{-2}$, which means that the highest values in the figure correspond to around 20% of the total variability.

https://doi.org/10.5194/egusphere-2023-653
Preprint. Discussion started: 11 April 2023

3.3 Influence of North Atlantic Heat Inertia on Extremely Warm European Summers

To test this causal relationship between ocean inertia and extremely warm European summers, we analyze the ocean heat content, which influences the temperature gradient between the ocean and atmosphere and thus alters the rate of heat exchange and is therefore a driver for the ocean-atmosphere heat flux. Here, we investigate anomalies of the 0-700m averaged, 5-10 year bandpass-filtered ocean heat content (Fig. 3a).

Starting around three years prior to extremely warm European summers, ocean heat content anomalies change from negative to positive all along the North Atlantic current, indicating an accumulation of heat in northern part of the subtropical gyre. For lag 0, these anomalies reach up to 25% of the total variability of the ocean heat content.

The ocean heat content is controlled by the meridional ocean heat transport, which is the movement of heat energy from one region of the ocean to another and can lead to changes in the ocean heat content in different regions over time. Here, further insight into the dynamics of the North Atlantic subtropical and subpolar region is provided by the 5-10 year bandpass-filtered ocean heat transport and its decomposition into a gyre- and meridional circulation part (Fig. 3b). The anomalies of the 5-10 year bandpass-filtered ocean heat transport reveals positive anomalies of the meridional heat transport around 20°N from 2 years prior to extremely warm summers onward. A substantial proportion of these positive anomalies of the meridional heat transport is not compensated by the heat released from the ocean heat transport divergence at e.g. 40°N. Here, due to the increased net heat transport around 40°N, the ocean heat content in that region will increase, leading to the previously described accumulation of ocean heat content. The accumulated heat is released at lag 0, mainly through the gyre ocean heat transport around 65°N. Altering the temperature gradient between the ocean and the atmosphere, this heat release matches in turn with the positive ocean-atmosphere heat flux anomaly around 50-70°N (Fig. 2).

The ocean heat transport is influenced by the direction and strength of the horizontal oceanic currents that transport heat, characterized by the barotropic stream function. Specifically, the barotropic stream function provides further knowledge about the boundary between the subtropical and subpolar gyre (Fig. 3c). Here, changes in the barotropic stream function can alter the path of ocean currents, leading to changes in the direction and magnitude of heat transport, and ultimately affecting the ocean heat content in different regions. Starting from 3 years prior to an extremely warm European summer, negative anomalies of the barotropic stream function occur in the northern part of the subtropical gyre, indicating a North Atlantic current weaker than its normal state, leading to a smaller horizontal volume transport and a southward shifted subpolar gyre boundary around 3 years prior to an extremely warm summer. The anomalies of the barotropic stream function change sign to positive values about one year prior to extremely warm summers, indicating strengthening of the North Atlantic current and associated greater horizontal volume transport. Moreover, the North Atlantic current shifts by a few degrees north compared to the mean state, indicating a volume transport into higher latitudes via the North Atlantic current. This increased northern horizontal volume transport together with the transition of the ocean heat content indicates the accumulation of heat inertia along the northern branch of the subtropical gyre.

https://doi.org/10.5194/egusphere-2023-653
Preprint. Discussion started: 11 April 2023

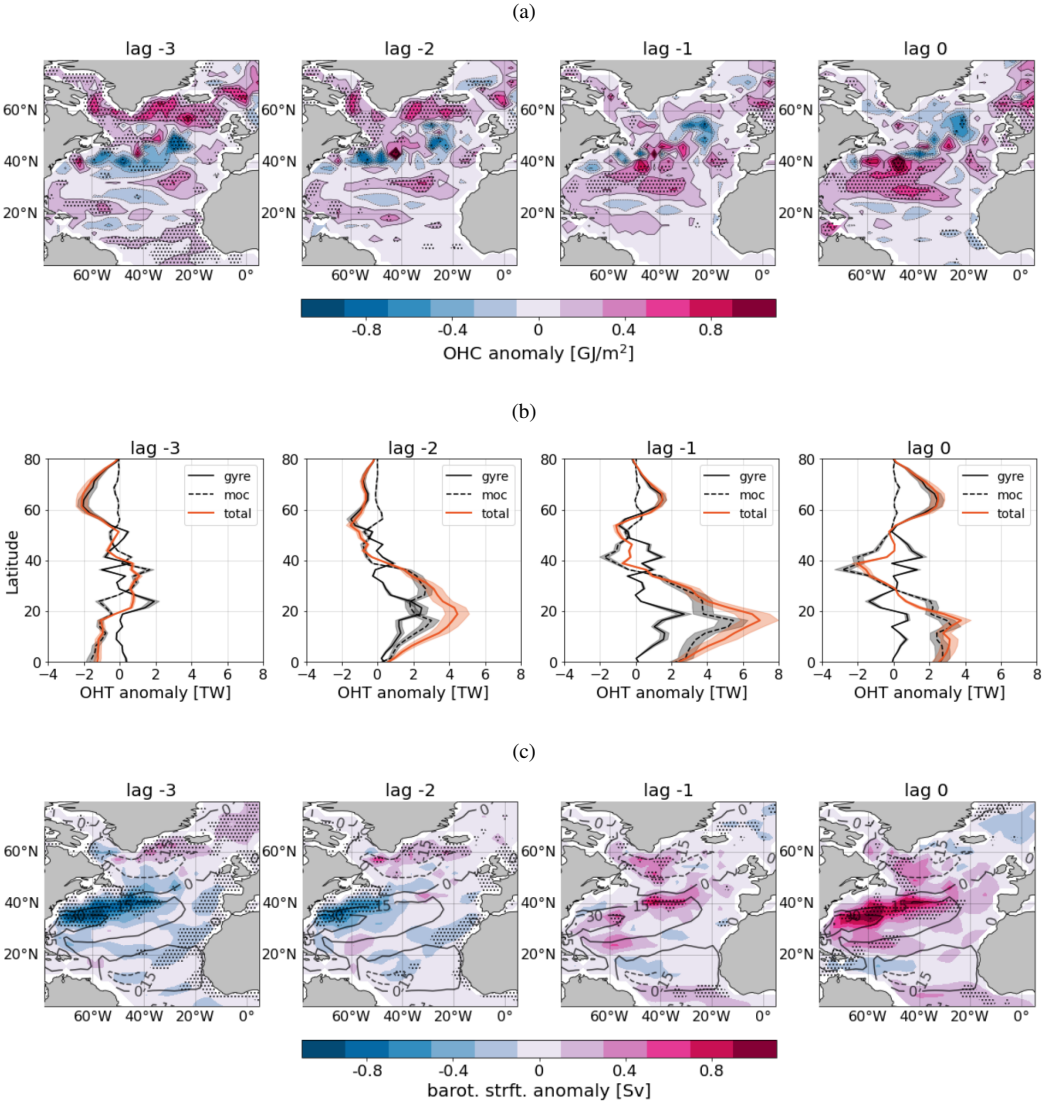

Figure 3. Extremely warm European summers and their relation to ocean quantities. (a) Upper 700m ocean heat content. Anomaly of 5-10 year bandpass-filtered ocean heat content variability in MPI-GE for different lags prior to extremely warm European summers, values given in GJm^{-2}. For comparison the standard deviation of the year-to-year variation is of the order of 4.3 GJm^{-2}, which means that the highest values in the figure correspond to around 25% of the total variability. (b) Ocean heat transport. Anomaly of 5-10 year bandpass-filtered ocean heat transport variability in MPI-GE for different lags prior to extremely warm European summers, values given in TW. For comparison the standard deviation of the year-to-year variation is of the order of 50 TW, which means that the highest values in the figure correspond to around 15% of the total variability. (c) Barotropic stream function. Anomaly of 5-10 year bandpass-filtered barotropic stream function variability in MPI-GE for different lags prior to extremely warm European summers, values given in Sv. Contour lines indicate the mean state of the barotropic stream function, values given in Sv. For comparison the standard deviation of the year-to-year variation is of the order of 8 Sv, which means that the highest values in the figure correspond to around 15% of the total variability. All lags are given in years. Dots (a, c) and shadings (b) denote significance at a 95% confidence level. Period 1950-2022.

https://doi.org/10.5194/egusphere-2023-653
Preprint. Discussion started: 11 April 2023

3.4 Atmospheric Pathway of North Atlantic Heat Inertia leading to Extremely Warm European Summers

Three years prior to an extremely warm European summer, heat accumulates along the North Atlantic current and is then released into the atmosphere during the extreme. Here, we explain how these processes trigger an atmospheric response that further influences the European summer climate.

The anomaly of the 5-10 year bandpass-filtered atmospheric temperature reveals positive temperature anomalies especially in higher latitudes around 50/60°N (Fig. 4a). Continuing the pathway of the ocean heat inertia into the atmosphere, these temperature anomalies fit to the previously located anomalies of the ocean heat transport. The transfer of heat from the ocean is so strong that its signal reaches up to 200 hPa altitude, with a peak in the range of 400-600 hPa. This warming of the tropospheric high latitudes provides a decrease of the meridional temperature gradient and results in a reduction of wind shear due to the thermal wind balance. This leads to a weakened jet stream in the years with extremely warm summers compared to years without heat extremes. In addition, the average position of the jet stream is shifted northward during extremely warm European summers, this northward shift indicates the advance of subtropical air masses into higher latitudes (Fig. 4; orange contour lines).

The structure of a Scandinavian Blocking can be identified for the 5-10 year bandpass-filtered mean sea level pressure between the simulated time series for years with and without extremely warm summers (Fig. 4b). The Scandinavian Blocking is known to drive heat extremes over Central Europe (Spensberger et al., 2020)), and confirms the connection between the sub-decadal variability of the North Atlantic and extremely warm summers over Central Europe. Additionally, the weakening of wind speeds during extremely warm European summers increases the probability of atmospheric blocking (Woollings et al., 2018), and in turn increases the likelihood of heat extremes (Kautz et al., 2022). Thus, we show how long-term North Atlantic heat inertia leads to accumulation of heat and an above average ocean-atmosphere heat flux, which in turn leads to the anticyclonic and atmospheric blocking conditions that, on daily to weekly timescales, drive European heat extremes.

https://doi.org/10.5194/egusphere-2023-653
Preprint. Discussion started: 11 April 2023

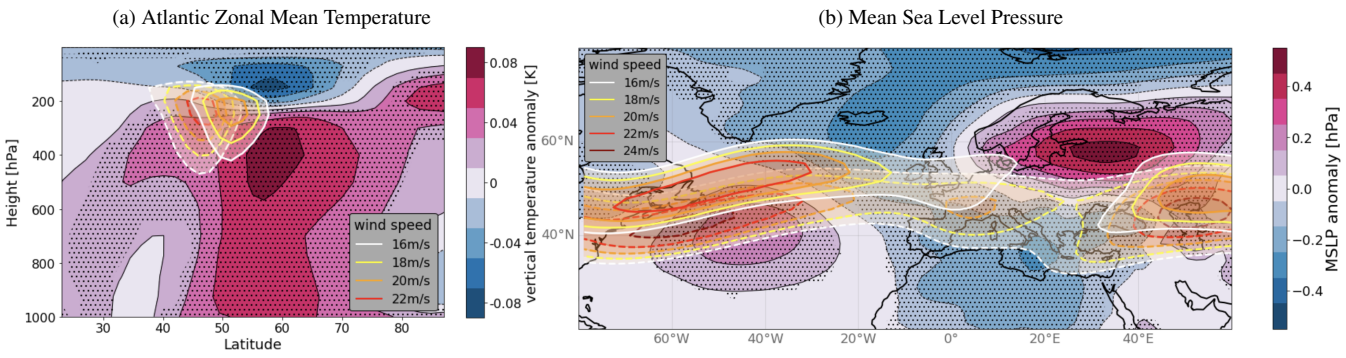

Figure 4. Extremely warm European summers and their atmospheric pathway. (a) Anomaly of 5-10 year bandpass-filtered Atlantic zonal mean temperature variability in MPI-GE during extremely warm European summers (lag0), values given in K. For comparison the standard deviation of the year-to-year variation is of the order of 0.3 K, which means that the highest values in the figure correspond to around 30% of the total variability. (b) Anomaly of 5-10 year bandpass-filtered mean sea level pressure variability in MPI-GE during extremely warm European summers (lag0), values given in hPa. For comparison the standard deviation of the year-to-year variation is of the order of 3 hPa, which means that the highest values in the figure correspond to around 15% of the total variability. The orange contour lines indicate the position of the jet stream (given by the mean zonal wind speed over 200-300 hPa) averaged over years showing an extremely warm European summer (solid line) and years showing no extremely warm summer (dashed line), values given in m/s. Dots denote significance at a 95% confidence level. Period 1950-2022.

4 Discussion and Conclusion

The North Atlantic heat inertia drives the occurrence of extremely warm summers over Central Europe on sub-decadal timescales. Starting several years prior, anomalies of the barotropic stream function, ocean heat content, as well as ocean heat transport result in ocean-atmosphere heat flux anomalies leading to extremely warm European summers.

Positive anomalies of the ocean heat content, together with an above average as well as more northern horizontal volume transport of the barotropic stream function lead to a stronger North Atlantic current and accumulation of heat content. This accumulated heat is released mainly through the ocean heat transport by the subpolar gyre during extremely warm European summers. The released heat in turn leads to a displacement of the jet stream and enhanced atmospheric blocking conditions.

https://doi.org/10.5194/egusphere-2023-653
Preprint. Discussion started: 11 April 2023

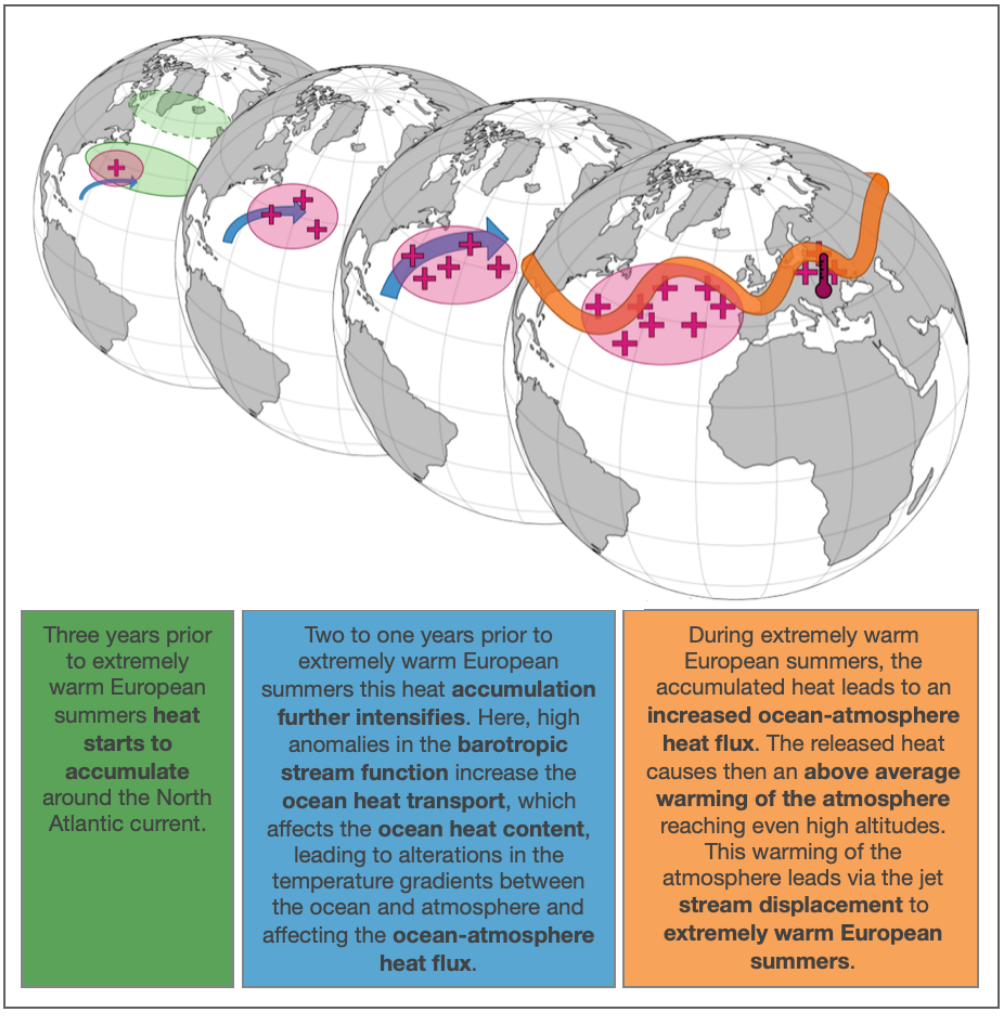

Figure 5. Schematic sketch illustrating the described mechanism.

Although we focus on three years prior to the extremely warm summers, there is evidence potentially linking this mechanism to a fully coupled atmosphere-ocean cycle in the North Atlantic evolving in a 7-10 year period. Such oscillating behavior has been identified in a number of quantities involving observed sea surface temperatures and Gulf Steam indices (Czaja and Marshall, 2001; McCarthy et al., 2018), or heat content and overturning stream functions (Martin et al., 2019), or for the North Atlantic Oscillation (NAO; Costa and Verdiere, 2002)). In fact, observations reveal that the European summer mean climate is ultimately connected to such a coupled atmosphere-ocean cycle (Müller et al., 2020). Comparable to our results, Martin et al. (2019) identified a similar atmosphere-ocean cycle using the MPI-ESM in the low-resolution setup. Extending our analysis up to 8 years prior to extremely warm summers is in line with their results, indicating the close relationship of the occurrence of extremely warm European summers with the sub-decadal North Atlantic atmosphere-ocean cycle (see Figures A1-A3).

https://doi.org/10.5194/egusphere-2023-653
Preprint. Discussion started: 11 April 2023

We find the coupled oscillation in the North Atlantic to prescribe extremely warm European summers on sub-decadal time scales. However, on this timescale other modes of oceanic variability may also be influential. Observed decadal teleconnections between the Pacific and North Atlantic have been demonstrated as shown e.g. in Müller et al. (2008). Global maps of heat flux during extremely warm European summers reveal negative anomalies within the tropical Pacific and patterns matching with the Pacific decadal variability (PDV; 90°-170°W/20°N), indicating an influence of other external drivers. However, a direct effect of ENSO on the sub-decadal occurrence of extremely warm European summers has not been found. Whether further climate modes have an impact on the proposed mechanism is beyond of the scope of this manuscript, and should be further explored.

Here, we focus on extremely warm European summers associated with the decadal atmosphere-ocean coupling in the North Atlantic. However, given that the coupled cycle appears over several years, we expect that there is not only an influence on the summertime, but also for other seasons and respective extreme conditions, and further variables relevant for heat extremes, such as the daily maximum temperature. Furthermore, the presented process of ocean heat distribution changes at multi-year lead times prior to an extreme event sets prospects to enhance the predictability of European climate and extremes. Multi-year prediction skill of European climate has been achieved on continental scale (Smith et al., 2020). However, an extension to predict extreme conditions has so far not fully been established (Borchert et al., 2019).

Moreover, the investigated sub-decadal extreme heat variability implies increased risk of heat-related socioeconomic and ecological impacts, in addition to year-to-year variability and rising temperatures due to increasing GHG concentrations. Due to the prominence of the sub-decadal variability and due to the severity of the impacts, a deeper understanding of the sub-decadal processes leading to such extremely warm summers is crucial for reducing the uncertainties in both attribution and prediction of high-impact events, which in turn facilitates preparedness and the efficiency of adaptation and mitigation efforts.

In sum, we present how sub-decadal processes in the North Atlantic coupled climate system drive the occurrence of extremely warm summers over Europe. We show that ocean inertia causes a heat content accumulation which precedes extremely warm European summers by several years. This accumulated heat is released in the year of the extreme, thereby influencing the atmospheric circulation in a way that favors the occurrence of extremely warm summers over Europe.

Data availability. Further simulation and download details for MPI-GE data can be found on our website (https://www.mpimet.mpg.de/en/grand-ensemble/). ERA5 data are available from the European Centre for Medium-Range Weather Forecasts (ECMWF) (https://www.ecmwf.int/en/forecasts/dataset/ecmwf-reanalysis-v5).

https://doi.org/10.5194/egusphere-2023-653
Preprint. Discussion started: 11 April 2023

Appendix A

A1 Barotropic Stream Function and Subpolar Gyre

The fact that no pronounced anomalies of the barotropic stream function can be found in the area of the subpolar gyre is probably related to the filter method we chose. The 5-10 year bandpass filter filters out all signals that occur on larger or smaller time scales. According to Nigam et al. (2018) the sub-polar gyre is subject to decadal variations of about 14 years and time scales which are not further relevant for our analysis.

A2 Noise of the Ocean Heat Content

The fact that the anomalies in the ocean heat content occurs in a more patchy and noisy pattern can probably be explained by the fact that the ocean heat content is also influenced by the atmospheric variability. Since the barotropic stream function is less influenced by atmospheric variability, the signal is clearer here.

A3 Link to fully coupled atmosphere-ocean cycle

Analyzing longer lags, in this case lag -7 to 0, prior to extremely warm European summers shows that the described mechanism can be seen as attached to a fully coupled atmosphere-ocean cycle evolving in a 7-10 year period (Figure A1-A3). Such oscillating behavior, without linkage to European summer climate, has been identified and described in previous studies (Czaja and Marshall, 2001; McCarthy et al., 2018; Martin et al., 2019). In Martin et al. (2019) a NAO-like wind-driven forcing steering dipolar ocean overturning anomalies are associated with a contraction and weakening of the sub-polar gyre (cf their figure 6). In the following years, the barotropic stream function reveals a poleward shift and a strengthening of the North Atlantic Current at the same time accumulates ocean heat content (cf. their figure 7). The barotropic stream function in MPI-GE prior to heat extremes similarly illustrates strengthening of the North Atlantic Current and accumulation of heat. For longer lags a phase reversal is apparent, similar to the oscillatory behavior of the coupling as described in Martin et al. (2019).

https://doi.org/10.5194/egusphere-2023-653
Preprint. Discussion started: 11 April 2023

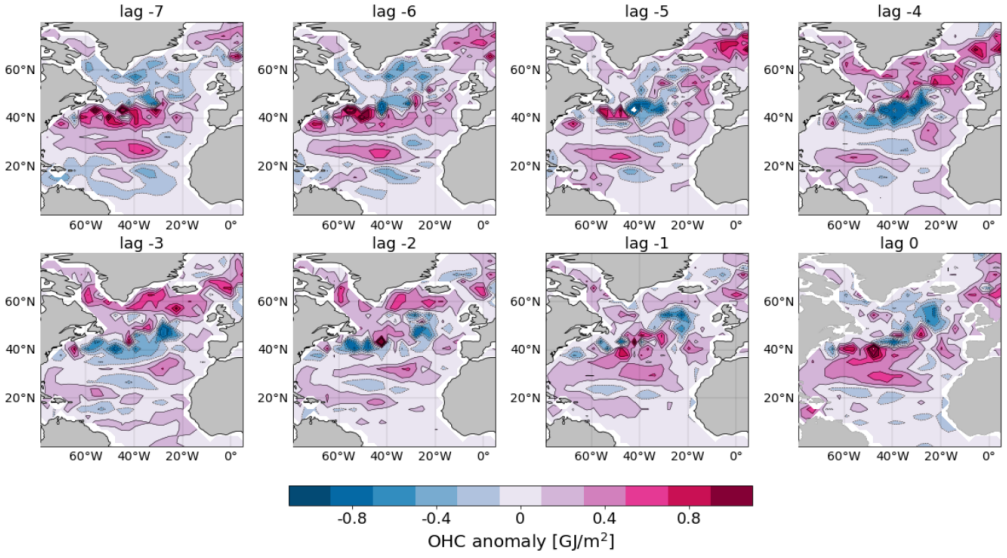

Figure A1. Shift of the ocean heat content signal. Anomaly of 5-10 year bandpass-filtered ocean heat content (0-700m/30-60°W) variability in MPI-GE for different lags prior to heat extremes. Period 1950-2022.

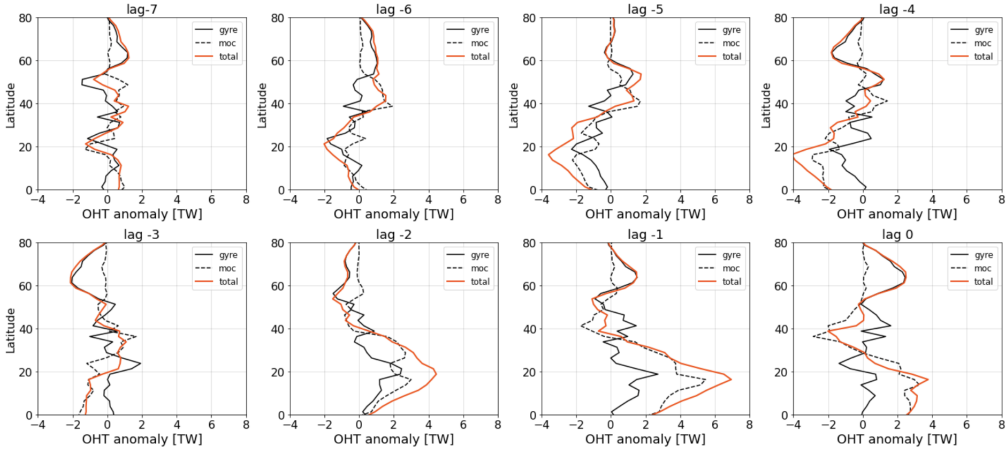

Figure A2. Shift of the ocean heat transport signal. Anomaly of 5-10 year bandpass-filtered ocean heat transport variability in MPI-GE for different lags prior to heat extremes. Period 1950-2022.

https://doi.org/10.5194/egusphere-2023-653
Preprint. Discussion started: 11 April 2023

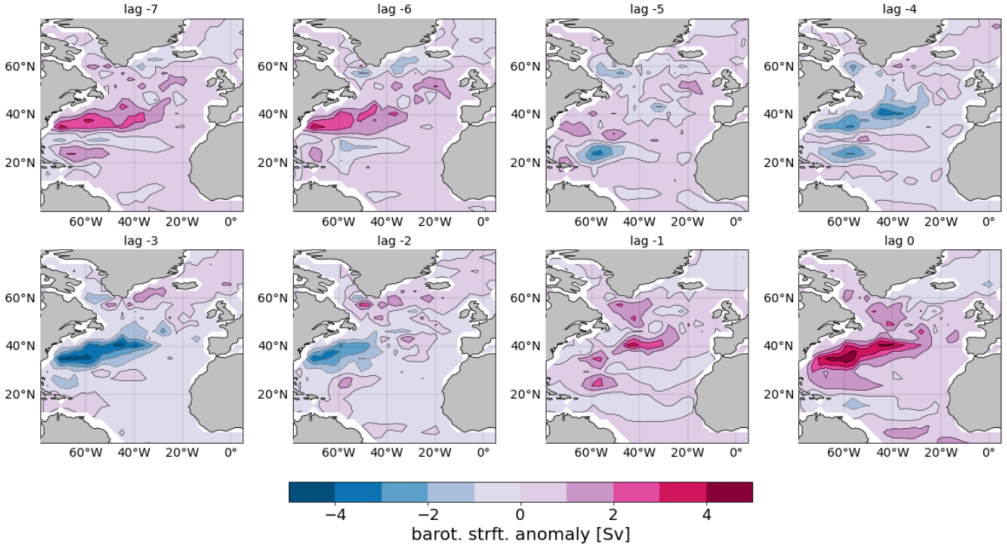

Figure A3. Shift of the barotropic stream function signal. Anomaly of 5-10 year bandpass-filtered barotropic stream function variability in MPI-GE for different lags prior to heat extremes. Period 1950-2022.

A4 Influence of the El Nino Southern Oscillation

Many studies have examined the influence of the El-Nino Southern Oscillation (ENSO) on European temperatures and also heat extremes (Martija-Díez et al., 2021). However, ENSO does not seem to play a dominant role for the mechanism studied here. On the one hand, the fraction of extremely warm European summers during the different ENSO phases (El-Nino, La-Nina, Neutral) is consistently low for different lags, so that no specific ENSO phase can be concretely linked to extremely warm European summers on sub-decadal time scales (Table A1). For this analysis, we defined ENSO phases by SSTs exceeding a threshold of $\pm$ one standard deviation in the Nino-3.4 region; however by checking other thresholds we verify that our conclusion is not threshold sensitive. Our statement that the extremely warm European summers are mainly driven by North Atlantic heat inertia and not ENSO is further supported by the proportion of extremely warm European summers during positive/negative anomalies of the barotropic stream function in the North Atlantic. Here, a clear correlation between both can be seen for different lags. While in lag 0 the extremely warm summers are mainly associated with positive anomalies of the barotropic stream function, these are in lag -4 mainly associated with negative anomalies of the barotropic stream function. Furthermore, for our study, no specific ENSO phase seem to be linked to specify anomalies of the barotropic stream function. In addition, the heat flux anomalies during extremely warm European summers show no typical ENSO pattern in the Nino-3.4 region (Fig. 2b). However, positive anomalies matching the North Pacific Index (NPI) could be found around 90°-170°W/20°N, indicating an influence of external drivers that, although beyond of the scope of this study, should be further explored.

https://doi.org/10.5194/egusphere-2023-653
Preprint. Discussion started: 11 April 2023

Table A1. Fraction of events that coincide with extremely warm European summers in MPI-GE. Period 1950-2022. The percentages are given by the ratio between the number of events (e.g. El-Nino events) during extremely warm European summers and the number of all occurring events.

	Fraction of events that coincide with an extremely warm European summer [%]		
	Lag -4	Lag -2	Lag 0
El-Nino events	9.1	8.3	7.5
neutral events	8.2	8.2	8.3
La-Nina events	7.2	7.7	8.0
positive barotropic stream function anomaly	4.5	7.1	13.2
negative barotropic stream function anomaly	11.7	9.2	3.0

Author contributions. L.H. did the analysis in correspondence with W.A.M., L.S.G., and D.M. and wrote the initial version of the manuscript. All authors commented on the manuscript. W.A.M., L.S.G., and D.M. provided guidance on the overall direction of the work.

Competing interests. The authors declare no competing financial interests.

Acknowledgements. This work was funded by the International Max Planck Research School on Earth System Modelling (IMPRS-ESM; L.H.), the ClimXtreme project DecHeat (Grant number 01LP1901F; L.S.G., W.A.M.), the European Union's Horizon Europe Framework Programme under the Marie Skłodowska-Curie grant agreement (101064940; L.S.G.), and the JPI Oceans NextG-Climate Science-ROADMAP project (01LP2002A; D.M.). We thank Luis Kornblueh, Jürgen Kröger, and Michael Botzet for producing the MPI-GE simulations we used for our analysis, Rohit Ghosh for providing the MPI-GE ocean heat transport data we used for our analysis, and Johann Jungclaus for reviewing the manuscript at an earlier stage. Furthermore, we acknowledge the Swiss National Computing Centre (CSCS) and the German Climate Computing Center (DKRZ) for providing the necessary computational resources.

https://doi.org/10.5194/egusphere-2023-653
Preprint. Discussion started: 11 April 2023

References

Årthun, M., Kolstad, E. W., Eldevik, T., and Keenlyside, N. S.: Time Scales and Sources of European Temperature Variability, Geophysical Research Letters, 45, 3597–3604, https://doi.org/10.1002/2018gl077401, 2018.

Borchert, L. F., Pohlmann, H., Baehr, J., Neddermann, N.-C., Suarez-Gutierrez, L., and Müller, W. A.: Decadal Predictions of the Probability of Occurrence for Warm Summer Temperature Extremes, 46, 14 042–14 051, https://doi.org/10.1029/2019gl085385, 2019.

Callahan, C. W. and Mankin, J. S.: Globally unequal effect of extreme heat on economic growth, Science Advances, 8, https://doi.org/10.1126/sciadv.add3726, 2022.

Cane, M. A., Clement, A. C., Murphy, L. N., and Bellomo, K.: Low-Pass Filtering, Heat Flux, and Atlantic Multidecadal Variability, Journal of Climate, 30, 7529–7553, https://doi.org/10.1175/jcli-d-16-0810.1, 2017.

Ceglar, A., Zampieri, M., Toreti, A., and Dentener, F.: Observed Northward Migration of Agro-Climate Zones in Europe Will Further Accelerate Under Climate Change, Earth's Future, 7, 1088–1101, https://doi.org/10.1029/2019ef001178, 2019.

Costa, E. D. D. and Verdiere, A. C. D.: The 7.7-year North Atlantic Oscillation, Quarterly Journal of the Royal Meteorological Society, 128, 797–817, https://doi.org/10.1256/0035900021643692, 2002.

Czaja, A. and Marshall, J.: Observations of atmosphere-ocean coupling in the North Atlantic, Quarterly Journal of the Royal Meteorological Society, 127, 1893–1916, https://doi.org/10.1002/qj.49712757603, 2001.

Fischer, E. M. and Schär, C.: Future changes in daily summer temperature variability: driving processes and role for temperature extremes, Climate Dynamics, 33, 917–935, https://doi.org/10.1007/s00382-008-0473-8, 2008.

Fischer, E. M., Rajczak, J., and Schär, C.: Changes in European summer temperature variability revisited, Geophysical Research Letters, 39, n/a–n/a, https://doi.org/10.1029/2012gl052730, 2012.

Gao, M., Yang, J., Gong, D., Shi, P., Han, Z., and Kim, S.-J.: Footprints of Atlantic Multidecadal Oscillation in the Low-Frequency Variation of Extreme High Temperature in the Northern Hemisphere, Journal of Climate, 32, 791–802, https://doi.org/10.1175/jcli-d-18-0446.1, 2019.

Gasparrini, A., Guo, Y., Hashizume, M., Kinney, P. L., Petkova, E. P., Lavigne, E., Zanobetti, A., Schwartz, J. D., Tobias, A., Leone, M., Tong, S., Honda, Y., Kim, H., and Armstrong, B. G.: Temporal Variation in Heat–Mortality Associations: A Multicountry Study, Environmental Health Perspectives, 123, 1200–1207, https://doi.org/10.1289/ehp.1409070, 2015.

Ghil, M., Allen, M. R., Dettinger, M. D., Ide, K., Kondrashov, D., Mann, M. E., Robertson, A. W., Saunders, A., Tian, Y., Varadi, F., and Yiou, P.: Advanced spectral methods for climatic time series, Reviews of Geophysics, 40, https://doi.org/10.1029/2000rg000092, 2002.

Ghosh, R., Müller, W. A., Baehr, J., and Bader, J.: Impact of observed North Atlantic multidecadal variations to European summer climate: a linear baroclinic response to surface heating, Climate Dynamics, 48, 3547–3563, https://doi.org/10.1007/s00382-016-3283-4, 2016.

Giorgetta, M. A., Jungclaus, J., Reick, C. H., Legutke, S., Bader, J., Böttinger, M., Brovkin, V., Crueger, T., Esch, M., Fieg, K., Glushak, K., Gayler, V., Haak, H., Hollweg, H.-D., Ilyina, T., Kinne, S., Kornblueh, L., Matei, D., Mauritsen, T., Mikolajewicz, U., Mueller, W., Notz, D., Pithan, F., Raddatz, T., Rast, S., Redler, R., Roeckner, E., Schmidt, H., Schnur, R., Segschneider, J., Six, K. D., Stockhause, M., Timmreck, C., Wegner, J., Widmann, H., Wieners, K.-H., Claussen, M., Marotzke, J., and Stevens, B.: Climate and carbon cycle changes from 1850 to 2100 in MPI-ESM simulations for the Coupled Model Intercomparison Project phase 5, Journal of Advances in Modeling Earth Systems, 5, 572–597, https://doi.org/10.1002/jame.20038, 2013.

https://doi.org/10.5194/egusphere-2023-653
Preprint. Discussion started: 11 April 2023

Hersbach, H., Bell, B., Berrisford, P., Biavati, G., Horányi, A., Muñoz Sabater, J., Nicolas, J., Peubey, C., Radu, R., Rozum, I., Schepers, D., Simmons, A., Soci, C., Dee, D., and Thépaut, J.-N.: ERA5 hourly data on pressure levels from 1959 to present, Copernicus Climate Change Service (C3S) Climate Data Store (CDS), https://doi.org/10.24381/cds.bd0915c6, 2018.

Horton, D. E., Johnson, N. C., Singh, D., Swain, D. L., Rajaratnam, B., and Diffenbaugh, N. S.: Contribution of changes in atmospheric circulation patterns to extreme temperature trends, Nature, 522, 465–469, https://doi.org/10.1038/nature14550, 2015.

Kautz, L.-A., Martius, O., Pfahl, S., Pinto, J. G., Ramos, A. M., Sousa, P. M., and Woollings, T.: Atmospheric blocking and weather extremes over the Euro-Atlantic sector – a review, Weather and Climate Dynamics, 3, 305–336, https://doi.org/10.5194/wcd-3-305-2022, 2022.

Li, M., Yao, Y., Simmonds, I., Luo, D., Zhong, L., and Chen, X.: Collaborative impact of the NAO and atmospheric blocking on European heatwaves, with a focus on the hot summer of 2018, Environmental Research Letters, 15, 114 003, https://doi.org/10.1088/1748-9326/aba6ad, 2020.

Maher, N., Milinski, S., Suarez-Gutierrez, L., Botzet, M., Dobrynin, M., Kornblueh, L., Kröger, J., Takano, Y., Ghosh, R., Hedemann, C., Li, C., Li, H., Manzini, E., Notz, D., Putrasahan, D., Boysen, L., Claussen, M., Ilyina, T., Olonscheck, D., Raddatz, T., Stevens, B., and Marotzke, J.: The Max Planck Institute Grand Ensemble: Enabling the Exploration of Climate System Variability, Journal of Advances in Modeling Earth Systems, 11, 2050–2069, https://doi.org/10.1029/2019ms001639, 2019.

Martija-Díez, M., Rodríguez-Fonseca, B., and López-Parages, J.: "ENSO Influence on Western European summer and fall Temperatures", Journal of Climate, pp. 1–51, https://doi.org/10.1175/jcli-d-20-0808.1, 2021.

Martin, T., Reintges, A., and Latif, M.: Coupled North Atlantic Subdecadal Variability in CMIP5 Models, Journal of Geophysical Research: Oceans, 124, 2404–2417, https://doi.org/10.1029/2018jc014539, 2019.

Mauritsen, T., Stevens, B., Roeckner, E., Crueger, T., Esch, M., Giorgetta, M., Haak, H., Jungclaus, J., Klocke, D., Matei, D., Mikolajewicz, U., Notz, D., Pincus, R., Schmidt, H., and Tomassini, L.: Tuning the climate of a global model, Journal of Advances in Modeling Earth Systems, 4, n/a–n/a, https://doi.org/10.1029/2012ms000154, 2012.

McCarthy, G. D., Joyce, T. M., and Josey, S. A.: Gulf Stream Variability in the Context of Quasi-Decadal and Multidecadal Atlantic Climate Variability, Geophysical Research Letters, 45, https://doi.org/10.1029/2018gl079336, 2018.

Meehl, G. A. and Tebaldi, C.: More Intense, More Frequent, and Longer Lasting Heat Waves in the 21st Century, Science, 305, 994–997, https://doi.org/10.1126/science.1098704, 2004.

Müller, W. A., Frankignoul, C., and Chouaib, N.: Observed decadal tropical Pacific–North Atlantic teleconnections, Geophysical Research Letters, 35, https://doi.org/10.1029/2008gl035901, 2008.

Müller, W. A., Borchert, L., and Ghosh, R.: Observed Subdecadal Variations of European Summer Temperatures, 47, https://doi.org/10.1029/2019gl086043, 2020.

Nigam, S., Ruiz-Barradas, A., and Chafik, L.: Gulf Stream Excursions and Sectional Detachments Generate the Decadal Pulses in the Atlantic Multidecadal Oscillation, Journal of Climate, 31, 2853–2870, https://doi.org/10.1175/jcli-d-17-0010.1, 2018.

Qasmi, S., Sanchez-Gomez, E., Ruprich-Robert, Y., Boé, J., and Cassou, C.: Modulation of the Occurrence of Heatwaves over the Euro-Mediterranean Region by the Intensity of the Atlantic Multidecadal Variability, Journal of Climate, 34, 1099–1114, https://doi.org/10.1175/jcli-d-19-0982.1, 2021.

Reintges, A., Latif, M., and Park, W.: Sub-decadal North Atlantic Oscillation variability in observations and the Kiel Climate Model, Climate Dynamics, 48, 3475–3487, https://doi.org/10.1007/s00382-016-3279-0, 2016.

Ribeiro, A. F. S., Russo, A., Gouveia, C. M., Páscoa, P., and Zscheischler, J.: Risk of crop failure due to compound dry and hot extremes estimated with nested copulas, Biogeosciences, 17, 4815–4830, https://doi.org/10.5194/bg-17-4815-2020, 2020.

https://doi.org/10.5194/egusphere-2023-653
Preprint. Discussion started: 11 April 2023

Ruiter, M. C., Couasnon, A., Homberg, M. J. C., Daniell, J. E., Gill, J. C., and Ward, P. J.: Why We Can No Longer Ignore Consecutive Disasters, Earth's Future, 8, https://doi.org/10.1029/2019ef001425, 2020.

Saeed, S., Lipzig, N. V., Müller, W. A., Saeed, F., and Zanchettin, D.: Influence of the circumglobal wave-train on European summer precipitation, 43, 503–515, https://doi.org/10.1007/s00382-013-1871-0, 2013.

Schär, C., Vidale, P. L., Lüthi, D., Frei, C., Häberli, C., Liniger, M. A., and Appenzeller, C.: The role of increasing temperature variability in European summer heatwaves, Nature, 427, 332–336, https://doi.org/10.1038/nature02300, 2004.

Seneviratne, Koster, R. D., Guo, Z., Dirmeyer, P. A., Kowalczyk, E., Lawrence, D., Liu, P., Mocko, D., Lu, C.-H., Oleson, K. W., and Verseghy, D.: Soil Moisture Memory in AGCM Simulations: Analysis of Global Land–Atmosphere Coupling Experiment (GLACE) Data, Journal of Hydrometeorology, 7, 1090–1112, https://doi.org/10.1175/jhm533.1, 2006.

Seneviratne, Zhang, X., Adnan, M., Badi, W., Dereczynski, C., A. Di Luca, S. Ghosh, I. I. J. K. S. L. F. O. I. P. M. S. S. V.-S. M. W., and Zhou, B.: Weather and Climate Extreme Events in a Changing Climate. In Climate Change 2021: The Physical Science Basis. Contribution of Working Group I to the Sixth Assessment Report of the Intergovernmental Panel on Climate Change, Cambridge University Press, Cambridge, United Kingdom and New York, NY, USA, https://doi.org/doi:10.1017/9781009157896.013, 2021.

Smith, D. M., Scaife, A. A., Eade, R., Athanasiadis, P., Bellucci, A., Bethke, I., Bilbao, R., Borchert, L. F., Caron, L.-P., Counillon, F., Danabasoglu, G., Delworth, T., Doblas-Reyes, F. J., Dunstone, N. J., Estella-Perez, V., Flavoni, S., Hermanson, L., Keenlyside, N., Kharin, V., Kimoto, M., Merryfield, W. J., Mignot, J., Mochizuki, T., Modali, K., Monerie, P.-A., Müller, W. A., Nicolí, D., Ortega, P., Pankatz, K., Pohlmann, H., Robson, J., Ruggieri, P., Sospedra-Alfonso, R., Swingedouw, D., Wang, Y., Wild, S., Yeager, S., Yang, X., and Zhang, L.: North Atlantic climate far more predictable than models imply, Nature, 583, 796–800, https://doi.org/10.1038/s41586-020-2525-0, 2020.

Spensberger, C., Madonna, E., Boettcher, M., Grams, C. M., Papritz, L., Quinting, J. F., Röthlisberger, M., Sprenger, M., and Zschenderlein, P.: Dynamics of concurrent and sequential Central European and Scandinavian heatwaves, Quarterly Journal of the Royal Meteorological Society, 146, 2998–3013, https://doi.org/10.1002/qj.3822, 2020.

Suarez-Gutierrez, L., Li, C., Müller, W. A., and Marotzke, J.: Internal variability in European summer temperatures at 1.5 °C and 2 °C of global warming, 13, 064 026, https://doi.org/10.1088/1748-9326/aaba58, 2018.

Suarez-Gutierrez, L., Müller, W. A., Li, C., and Marotzke, J.: Dynamical and thermodynamical drivers of variability in European summer heat extremes, Climate Dynamics, 54, 4351–4366, https://doi.org/10.1007/s00382-020-05233-2, 2020a.

Suarez-Gutierrez, L., Müller, W. A., Li, C., and Marotzke, J.: Hotspots of extreme heat under global warming, Climate Dynamics, 55, 429–447, https://doi.org/10.1007/s00382-020-05263-w, 2020b.

Suarez-Gutierrez, L., Milinski, S., and Maher, N.: Exploiting large ensembles for a better yet simpler climate model evaluation, Climate Dynamics, 57, 2557–2580, https://doi.org/10.1007/s00382-021-05821-w, 2021.

Vicedo-Cabrera, A. M., Scovronick, N., Sera, F., Royé, D., Schneider, R., Tobias, A., Astrom, C., Guo, Y., Honda, Y., Hondula, D. M., Abrutzky, R., Tong, S., de Sousa Zanotti Stagliorio Coelho, M., Saldiva, P. H. N., Lavigne, E., Correa, P. M., Ortega, N. V., Kan, H., Osorio, S., Kyselý, J., Urban, A., Orru, H., Indermitte, E., Jaakkola, J. J. K., Ryti, N., Pascal, M., Schneider, A., Katsouyanni, K., Samoli, E., Mayvaneh, F., Entezari, A., Goodman, P., Zeka, A., Michelozzi, P., de'Donato, F., Hashizume, M., Alahmad, B., Diaz, M. H., Valencia, C. D. L. C., Overcenco, A., Houthuijs, D., Ameling, C., Rao, S., Ruscio, F. D., Carrasco-Escobar, G., Seposo, X., Silva, S., Madureira, J., Holobaca, I. H., Fratianni, S., Acquaotta, F., Kim, H., Lee, W., Iniguez, C., Forsberg, B., Ragettli, M. S., Guo, Y. L. L., Chen, B. Y., Li, S., Armstrong, B., Aleman, A., Zanobetti, A., Schwartz, J., Dang, T. N., Dung, D. V., Gillett, N., Haines, A., Mengel, M., Huber, V., and Gasparrini, A.: The burden of heat-related mortality attributable to recent human-induced climate change, Nature Climate Change, 11, 492–500, https://doi.org/10.1038/s41558-021-01058-x, 2021.

https://doi.org/10.5194/egusphere-2023-653
Preprint. Discussion started: 11 April 2023

Vogel, M. M., Orth, R., Cheruy, F., Hagemann, S., Lorenz, R., Hurk, B. J. J. M., and Seneviratne, S. I.: Regional amplification of projected changes in extreme temperatures strongly controlled by soil moisture-temperature feedbacks, Geophysical Research Letters, 44, 1511–1519, https://doi.org/10.1002/2016gl071235, 2017.

von Storch, H. and Zwiers, F. W.: Statistical Analysis in Climate Research, Cambridge University Press, https://doi.org/10.1017/cbo9780511612336, 1984.

Woollings, T., Barnes, E., Hoskins, B., Kwon, Y.-O., Lee, R. W., Li, C., Madonna, E., McGraw, M., Parker, T., Rodrigues, R., Spensberger, C., and Williams, K.: Daily to Decadal Modulation of Jet Variability, Journal of Climate, 31, 1297–1314, https://doi.org/10.1175/jcli-d-17-0286.1, 2018.